ARTICLES
PUBLISHED ONLINE: 25 OCTOBER 2009 | DOI: 10.1038/NMAT2558
nature materials

# Nanofibrous biologic laminates replicate the form and function of the annulus fibrosus

Nandan L. Nerurkar, Brendon M. Baker, Sounok Sen, Emily E. Wible, Dawn M. Elliott and Robert L. Mauck*

**Successful engineering of load-bearing tissues requires recapitulation of their complex mechanical functions. Given the intimate relationship between function and form, biomimetic materials that replicate anatomic form are of great interest for tissue engineering applications. However, for complex tissues such as the annulus fibrosus, scaffolds have failed to capture their multi-scale structural hierarchy. Consequently, engineered tissues have yet to reach functional equivalence with their native counterparts. Here, we present a novel strategy for annulus fibrosus tissue engineering that replicates this hierarchy with anisotropic nanofibrous laminates seeded with mesenchymal stem cells. These scaffolds directed the deposition of an organized, collagen-rich extracellular matrix that mimicked the angle-ply, multi-lamellar architecture and achieved mechanical parity with native tissue after 10 weeks of *in vitro* culture. Furthermore, we identified a novel role for inter-lamellar shearing in reinforcing the tensile response of biologic laminates, a mechanism that has not previously been considered for these tissues.**

The annulus fibrosus is a multi-lamellar fibrocartilage that, together with the nucleus pulposus, forms the intervertebral disc, a soft tissue structure that transmits loads between vertebrae and permits motion of the spine. Function of the annulus fibrosus is predicated on a high degree of structural organization over multiple length scales: aligned bundles of collagen fibres reside within each lamella and the direction of alignment alternates from one lamella to the next by 30° above and below the transverse plane[1]. The resulting angle-ply laminate possesses pronounced mechanical anisotropy and nonlinearity[2]. Clinical treatments for disc degeneration are primarily palliative, demonstrating a need for tissue engineering strategies that restore physiologic function to the spine while alleviating lower back pain[3]. So far, numerous strategies have been proposed to engineer replacement tissues for the annulus fibrosus and the intervertebral disc[4]. However, these studies have failed to replicate the angle-ply microstructure that is necessary for proper mechanical function of the native tissue. Indeed, these studies have shown that in the absence of a scaffold that provides the appropriate structural—and perhaps mechanical—cues, cells are unable to spontaneously organize their extracellular matrix into highly specialized architectures such as that of the annulus fibrosus. Consequently, no engineered tissue has successfully achieved mechanical properties that are commensurate with the native tissue. Therefore, the overarching goal of the present work is to engineer a tissue that achieves functional parity with the annulus fibrosus by developing a strategy that mirrors the natural multi-scale organization of extracellular matrix within this tissue.

A successful strategy for the tissue engineering of load-bearing tissues must rely on the proper selection of biomaterial scaffolds, and their assembly into structures that replicate essential anatomic features of the tissue of interest[5,6]. Therefore, in this study, we used electrospun nanofibrous scaffolds seeded with mesenchymal stem cells (MSCs) to generate angle-ply multi-lamellar tissues that replicate the anatomic form of the annulus fibrosus. In contrast to scaffolds previously used for annulus fibrosus tissue engineering, which include hydrogels[7,8] and macroporous synthetic[9,10] and natural[11,12] polymers, electrospinning permits the formation of arrays of aligned polymeric nanofibres, serving as a template for the deposition of a unidirectionally organized extracellular matrix by resident cells[13]. In the present work, engineered bi-lamellar tissues reached mechanical equivalence with the annulus fibrosus after 10 weeks of *in vitro* culture and revealed a potential role for inter-lamellar shearing as a mechanism of tensile reinforcement for biologic laminates. In addition to advancing the field of annulus fibrosus tissue engineering, these findings provide insight into the relationship between form and function in biologic laminates, with implications for other orthopaedic and cardiovascular tissues.

To replicate the structural hierarchy of the annulus fibrosus, bi-lamellar tissue constructs were formed first as single lamellar tissues from aligned nanofibrous scaffolds seeded with MSCs, and then coupled into bilayers after two weeks of *in vitro* culture. MSCs were used in place of annulus fibrosus cells owing to the clinical limitations associated with the latter; specifically, it remains uncertain whether healthy cells can be isolated from degenerate discs, and isolation from healthy discs may result in donor site morbidity. In contrast, MSCs are multipotent and can be readily isolated from bone-marrow aspirate, making them an attractive cell source for engineering a broad range of tissues[14,15]. Planar sheets of scaffolds were fabricated by electrospinning poly($\varepsilon$-caprolactone) (PCL) onto a rotating mandrel to instill alignment among the collecting fibres. Mats of ~250 μm thickness were electrospun to match the natural lamellar thickness of the annulus fibrosus[16]. PCL was used owing to its slow degradation rate, its ability to be readily formed into nanofibres and its proven potential for *in vivo* application[17]. Moreover, we have recently shown that aligned electrospun PCL meshes mimic the mechanical anisotropy and nonlinearity of fibre-reinforced soft tissues, and undergo finite elastic deformations[18].

Rectangular scaffolds (5 mm × 30 mm) were excised from the nanofibrous mat with their long axis rotated 30° from the prevailing

McKay Orthopaedic Research Laboratory, University of Pennsylvania, 424 Stemmler Hall, 36th Street and Hamilton Walk, Philadelphia, Pennsylvania 19104-6081, USA. *e-mail: lemauck@mail.med.upenn.edu.

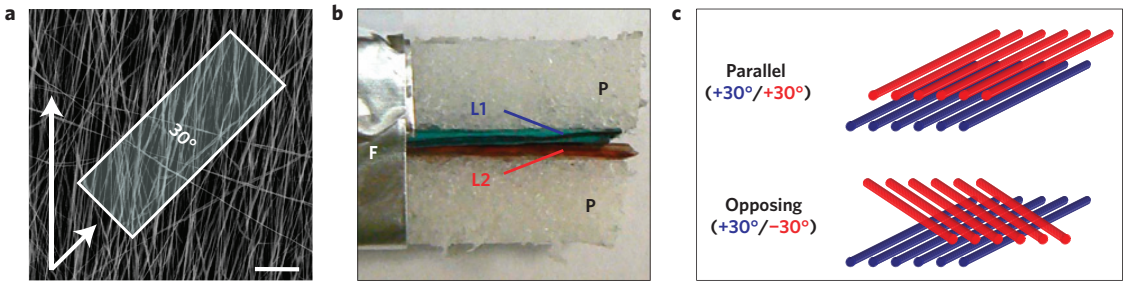


**Figure 1 | Fabrication of bi-lamellar tissue constructs. a**, Scaffolds were excised 30° from the prevailing fibre direction of electrospun nanofibrous mats to replicate the oblique collagen orientation within a single lamella of the annulus fibrosus. Scale bar: 25 μm. **b**, At zero weeks, MSC-seeded scaffolds were formed into bilayers between pieces of porous polypropylene and wrapped with a foil sleeve. P: porous polypropylene; F: foil; L1/2: lamella 1/2. **c**, Bilayers were oriented with either parallel (+30°/+30°) or opposing (+30°/−30°) fibre alignment relative to the long axis of the scaffold.

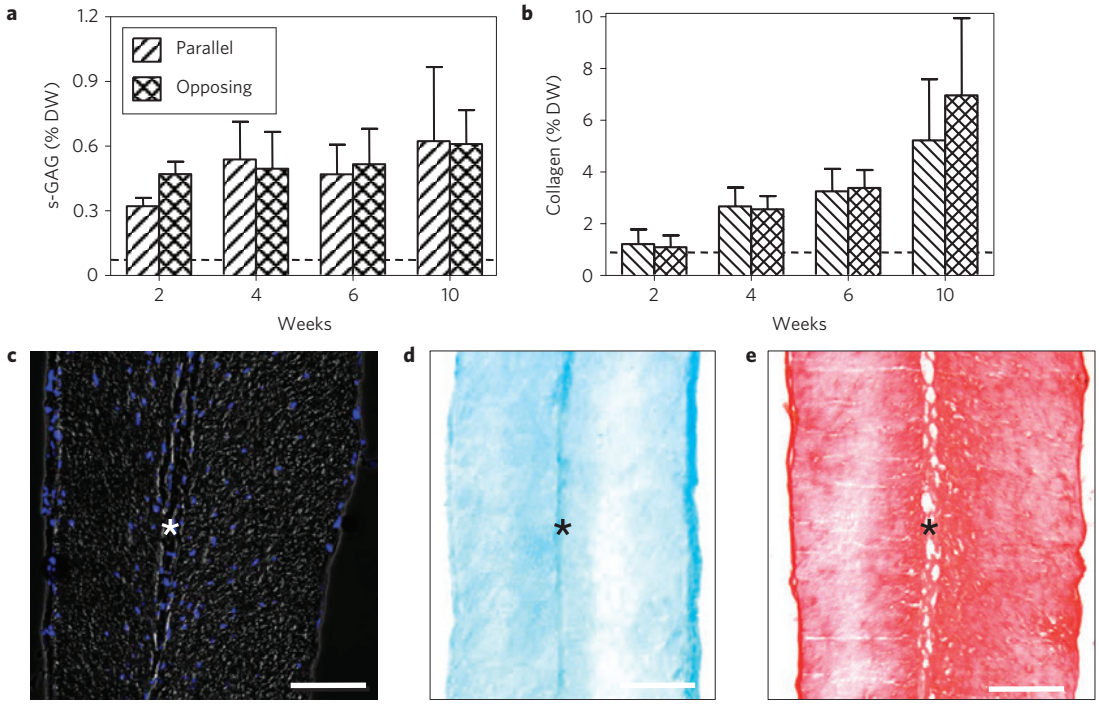


**Figure 2 | Elaboration of extracellular matrix within bilayers seeded with MSCs. a**,**b**, s-GAG (**a**) and collagen (**b**) content of parallel and opposing bilayers increased with culture duration ($p \leq 0.05$). There were no significant differences between parallel and opposing bilayers at any time point. DW: dry weight. The dashed line indicates content at zero weeks, when bilayers were formed. The error bars represent the standard deviation of the mean. **c**–**e**, DAPI (**c**), Alcian blue (**d**) and Picrosirius Red (**e**) staining of opposing bilayer cross-sections after 10 weeks of *in vitro* culture. The asterisk indicates inter-lamellar space. Scale bars: 200 μm (**c**), 250 μm (**d**,**e**).

fibre direction. This produces aligned scaffolds with a fibre angle (Fig. 1a) that reflects the oblique alignment of collagen fibres within a single lamella of the annulus fibrosus. These single-lamellar scaffolds were seeded with bovine MSCs and cultured *in vitro* in a medium formulation supportive of fibrocartilaginous differentiation[13,19]. After two weeks, lamellae were brought into apposition between pieces of porous polypropylene and wrapped with a foil sleeve (0 weeks, Fig. 1b). Bilayers were formed with the nanofibres in adjacent lamellae running either parallel at +30° (parallel) or in opposing directions of +30° and −30° (opposing, Fig. 1c). After two more weeks of culture, the external supports were removed and the laminates remained intact.

Biochemical analyses through 10 weeks of *in vitro* culture revealed significant accumulation of sulphated glycosaminoglycans (s-GAGs; Fig. 2a,d) and collagen (Fig. 2b,e), two of the primary extracellular components of the annulus fibrosus, within both parallel and opposing bilayers. In the two weeks preceding bilayer formation, cells began infiltrating through the thickness with a dense cell layer at the scaffold periphery (not shown). After bilayer formation, these outer cell layers fused in the contacting region between two lamellae, forming a thin inter-lamellar space that became more pronounced with culture duration (asterisks, Fig. 2c–e). Glycosaminoglycans and collagen were distributed throughout each lamella, and within this inter-lamellar space, indicating the successful formation of a biologic interface between the two layers (Fig. 2c,d). MSCs infiltrated into the scaffold, but remained most densely populated at the surfaces (Fig. 2e). No differences in cell, glycosaminoglycan or collagen quantity and localization were observed between parallel and opposing bilayers, nor were any differences observed compared to single-lamella constructs maintained under identical culture conditions (normalized to dry weight). This indicates that altering the direction of alignment of one lamella relative to the other did not affect cell biosynthesis and that culture in the thicker, two-lamella format did not diminish *in vitro* growth relative to single-lamella constructs. Despite abundant deposition of extracellular matrix

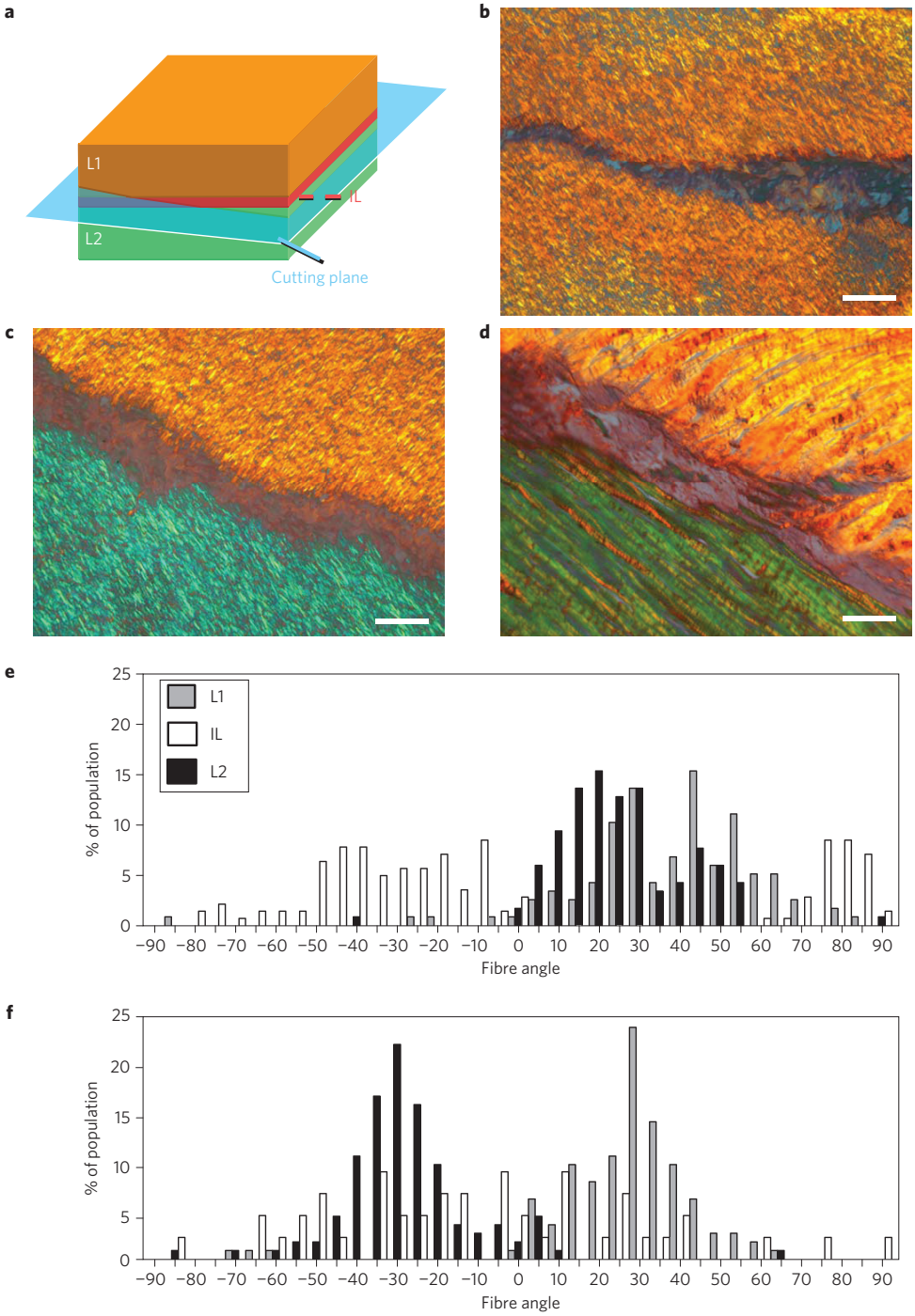


**Figure 3 | Angle-ply collagen alignment and orientation. a** Sections were collected obliquely across lamellae, stained with Picrosirius Red, and viewed under polarized light microscopy to visualize collagen organization. When viewed under crossed polarizers, birefringent intensity indicates the degree of alignment of the specimen, and the hue of birefringence indicates the direction of alignment. L1/2: lamella 1/2; IL: inter-lamellar space. **b**, After 10 weeks of *in vitro* culture, parallel bilayers contained co-aligned intra-lamellar collagen within each lamella. **c**,**d**, Opposing bilayers contained intra-lamellar collagen aligned along two opposing directions (**c**), successfully replicating the gross fibre orientation of native bovine annulus fibrosus (**d**). In engineered bilayers, as well as the native annulus fibrosus, a thin layer of disorganized (non-birefringent) collagen was observed at the lamellar interface. The distribution of collagen fibre orientations was determined by quantitative polarized light analysis[45]. Scale bars: 200 μm (**b**,**c**), 100 μm (**d**). **e**, Prominent peaks in fibre alignment were observed near 30° in both lamellae of parallel bilayers. **f**, In opposing bilayers, two fibre populations were observed, aligned along +30° and −30°.

molecules, collagen and glycosaminoglycan contents remained less than the native annulus fibrosus. It is possible that some form of mechanical stimulation[20–22] or *in vivo* implantation[23] may be necessary to generate native tissue composition in a clinically relevant time frame.

We next examined collagen organization in matured constructs. Parallel and opposing bilayers were visualized obliquely to observe collagen alignment simultaneously across layers (Fig. 3a). When stained for collagen and viewed by polarized light microscopy, intra-lamellar collagen was highly birefringent in both parallel

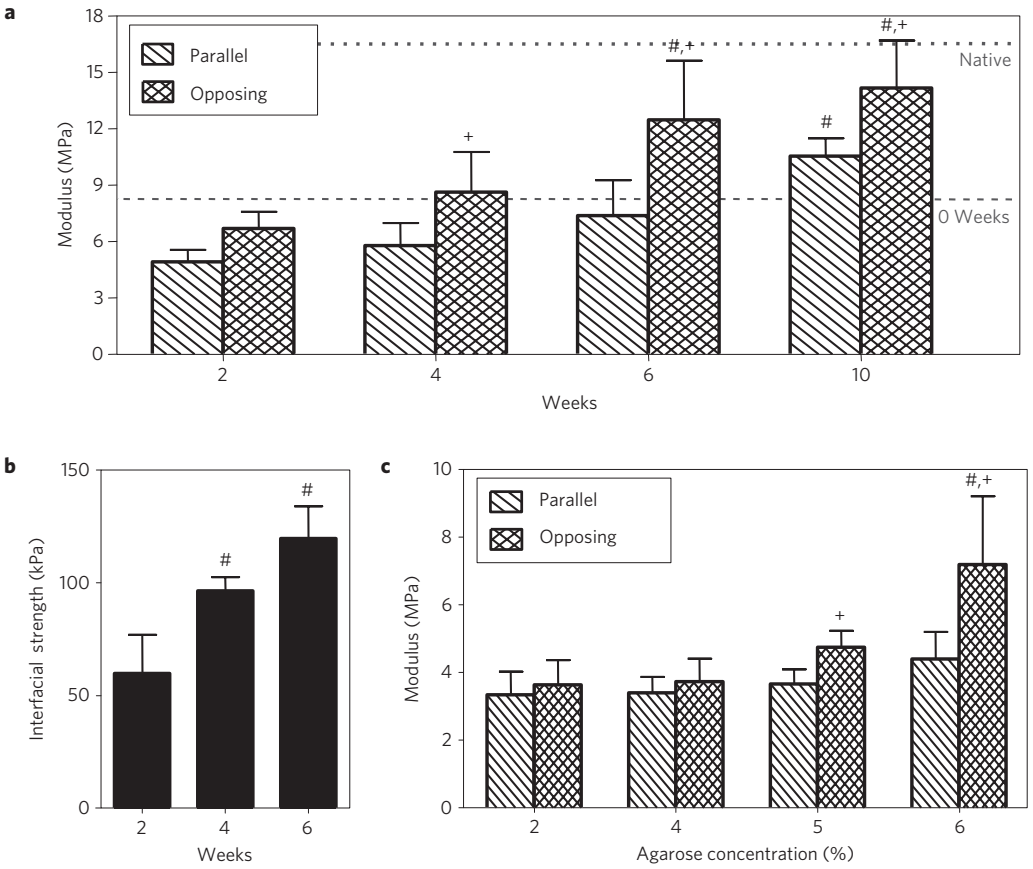


**Figure 4 | Relating inter-lamellar mechanics with the tensile response of biologic laminates. a**, Uniaxial tensile moduli of MSC-seeded parallel and opposing bilayers increased with *in vitro* culture duration, with opposing bilayers achieving significantly higher moduli than parallel bilayers from four weeks onward. # : $p \leq 0.05$ compared with single-lamellar modulus at zero weeks. + : $p \leq 0.05$ compared with parallel bilayers. Native: circumferential tensile modulus of native human annulus fibrosus[2]. **b**, Lap testing of MSC-seeded laminates showed increasing interface strength with *in vitro* culture duration. # : $p \leq 0.05$ compared with two weeks. **c**, To elucidate the role of interface properties on the tensile response of bilayers, uniaxial tensile testing was carried out on acellular bilayers formed from nanofibrous scaffolds bonded together by agarose of increasing concentrations. Increasing inter-lamellar agarose concentration—and hence inter-lamellar stiffness—significantly increased the tensile modulus of acellular opposing bilayers, but had no effect on the parallel bilayer group. # : $p \leq 0.05$ compared with orientation-matched 2% agarose. + : $p \leq 0.05$ compared with concentration-matched parallel bilayers. All error bars represent standard deviations of the mean.

(Fig. 3b) and opposing (Fig. 3c) bilayers, indicating that collagen was aligned with the underlying nanofibrous scaffold. Collagen deposited into the inter-lamellar region, however, was disorganized. As indicated by the hue of birefringence, intra-lamellar collagen was co-aligned within parallel bilayers and oriented along two opposing directions for opposing bilayers. Furthermore, collagen organization within opposing bilayers compared favourably to similarly prepared sections of annulus fibrosus (Fig. 3d), indicating successful replication of the multi-scale collagen architecture of the native tissue. Importantly, disorganized inter-lamellar matrix was also observed in the native annulus fibrosus, as has been shown previously[24]. Quantitative polarized light analysis confirmed co-alignment of intra-lamellar collagen in parallel bilayers, indicated by overlapping fibre populations (Fig. 3e) at approximately +30° from the long axis. However, fibre populations within opposing bilayers demonstrated two distinct peaks in orientation: +30° and −30° from the long axis. For both parallel and opposing bilayers, inter-lamellar matrix orientations were widely distributed with no single distinct peak, confirming lack of alignment in this region. Opposing bilayers present the first instance in which an engineered tissue has successfully replicated the angle-ply laminate architecture of the annulus fibrosus. Despite successful replication of principal architectural features, it is also apparent from the histologic comparison above that some intra-lamellar characteristics of collagen organization, such as crimp and fibril bundling, were not replicated by the engineered construct. At present, it is not known how MSCs can be induced to replicate these fine features, ubiquitous throughout connective tissues of the body. Nonetheless, an advanced understanding of how collagen crimp and fibre bundling arise during development, and how they can be recreated *in vitro*, may have an important role in the future of tissue engineering for load-bearing soft tissues.

We next determined whether replication of anatomic form translates to enhanced mechanical function of these biologic laminates. As the annulus fibrosus is subjected to large circumferential tensile stresses during *in vivo* compression of the intervertebral disc, a primary objective of this study was to generate an engineered tissue with a uniaxial tensile modulus of similar magnitude to the tensile modulus of the native tissue along its circumferential direction. For both parallel and opposing bilayers, tensile moduli increased with culture duration when compared with single-lamellar moduli at the time of bilayer formation (0 weeks, Fig. 4a). In the first few weeks after apposition, a reduction in modulus was observed due to swelling; stiffness steadily increased for both groups for all time points (not shown). Interestingly, opposing bilayer moduli were significantly greater than parallel bilayers by as early as four weeks, and remained higher through completion of the study at 10 weeks ($p \leq 0.05$). In fact, opposing ($14.2 \pm 2.5$ MPa)—but not

parallel (10.6 ± 0.9 MPa)—bilayers achieved a tensile modulus by 10 weeks that approximates the circumferential tensile modulus of the annulus fibrosus to within 15% (17.3 MPa; ref. 2). This is, so far, the closest an engineered tissue has come to matching the tensile properties of the annulus fibrosus.

The disparity in mechanical function between parallel and opposing bilayers, despite compositional equivalence, suggests that when the two fibre populations are combined in opposition, the resulting laminate is stiffer than if the same two fibre populations coincide. For this to be true, it is necessary that fibre populations interact across the interface, and do so in an orientation-dependent manner. As interaction across lamellae requires that they be bonded together, we next sought to determine the role of inter-lamellar matrix in the macroscopic tensile response of biologic laminates. As this stiffening effect was not observed initially, but instead developed with time in culture, it is likely that a sufficiently strong interface must exist for this reinforcement to occur. Therefore, we examined the evolution of interfacial strength over time by carrying out lap tests on MSC-seeded nanofibrous bilayers. To isolate the functional properties of the interface, intra-lamellar deformations were reduced by: (1) using thicker (1 mm) scaffolds and (2) aligning nanofibres parallel to the loading axis in both lamellae. Scaffolds of this size and orientation were two orders of magnitude stiffer than the interface, allowing direct measurement of interfacial properties with minimal intra-lamellar deformation. Indeed, failure occurred consistently at the interface. Interfacial strength increased by nearly threefold within the first six weeks after bilayer formation (Fig. 4b). This suggests that although after two weeks of *in vitro* culture, load can be transmitted across the inter-lamellar space, the strength of bonding continues to increase with culture duration. This supports the potential role for lamellar bonding in explaining the functional disparity between parallel and opposing bilayers.

It is well established from studies on fibre-reinforced materials, including electrospun scaffolds[25] and fibrous soft tissues such as the annulus fibrosus[26], that fibres re-orient under external forces towards the direction in which loads are applied. Therefore, in opposing bilayers, uniaxial tension induces clockwise fibre rotation in one lamella (L1, Fig. 5, top) while simultaneously inducing the fibres to rotate anticlockwise in the adjacent lamella (L2, Fig. 5). Fibre rotation along two opposing directions would require the movement of one lamella against the other, shearing the inter-lamellar space (IL, Fig. 5). Therefore, by enhancing the strength of bonding across the two lamellae, the inter-lamellar matrix may resist the local deformations associated with fibre re-orientation, thereby reinforcing the overall tensile response. However, in the case of parallel bilayers (Fig. 5, bottom), the fibres within the two lamellae reorient identically, and no shearing of the inter-lamellar space occurs. As the bonding strength between the two layers increases with culture duration, it is likely that at two weeks, no difference was observed between parallel and opposing bilayer moduli because the interface was weak and newly formed; however, with increasing culture duration, the disparity in bilayer tensile moduli increased owing to improved inter-lamellar bonding, generating a stronger resistance to inter-lamellar shearing.

This proposed mechanism is consistent with the stiffening of opposing bilayers relative to parallel bilayers, and a confirmatory acellular study was conducted to isolate the role of inter-lamellar bonding in the mechanical response of biomimetic laminates. This simpler system, which consisted of aligned electrospun lamellae bonded together by varying concentrations of agarose, permitted the variation of interfacial mechanics without the ambiguity introduced by cell-generated extracellular matrix. The tensile stiffness of agarose is of similar magnitude to the interfacial strength measured above (~100 kPa), and bonding strength can be

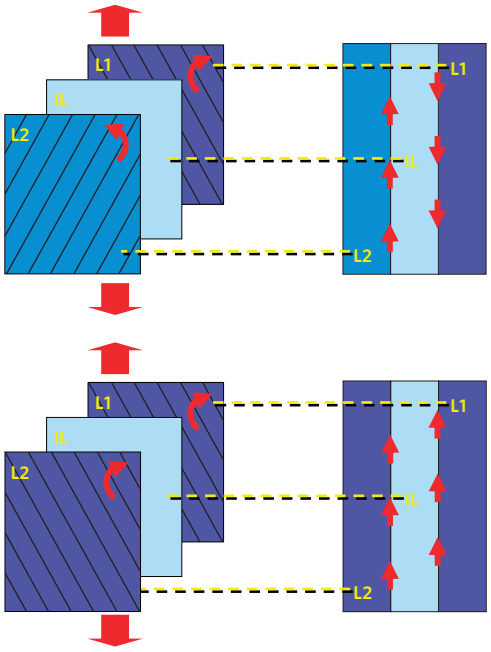


**Figure 5 | A novel mechanism for tensile reinforcement by inter-lamellar shearing of biologic laminates.** In opposing bilayers (top), fibres within each lamella reorient under uniaxial load by rotating (red curved arrows) towards the loading direction. The opposing direction of rotation between lamellae generates shearing of the inter-lamellar matrix. However, in parallel bilayers (bottom) fibres reorient identically in the two lamellae, and therefore do not shear the inter-lamellar space. L1/2: lamellae 1/2; IL: inter-lamellar space.

readily manipulated by altering the gel concentration. Consistent with the proposed mechanism (Fig. 5), opposing bilayer modulus increased with increasing agarose concentration ($p \leq 0.05$) and hence inter-lamellar bonding strength, whereas parallel bilayers were unchanged (Fig. 4c). It is notable that whereas the modulus of agarose alone increases only of the order of 0.1 MPa with increasing concentration from 2 to 6% (ref. 27), the opposing bilayer modulus increased by 3.5 MPa. Therefore, we conclude that the increase in opposing bilayer modulus results, not simply from the presence of stiffer inter-lamellar agarose (which would have produced similar changes in parallel bilayers), but specifically from an increased resistance to shearing as fibres reorient under load. These results confirm the importance of inter-lamellar shearing interactions in reinforcing the tensile response of angle-ply biologic laminates.

Given the structural similarity between opposing bilayers and the annulus fibrosus (Fig. 3c,d), it is reasonable to posit that such a mechanism of reinforcement is important for function of the annulus fibrosus as well. Although the structure, composition and function of its inter-lamellar matrix are not well defined, recent work suggests that each is quite complex. Elastin[24], lubricin[28] and collagen type VI (ref. 29) have been detected at lamellar boundaries and microscopy studies suggest that there may be an intricate network of fibrous channels bridging adjacent lamellae[30]. Functionally, however, much less is known about the inter-lamellar matrix of the annulus fibrosus. Recent work suggests that the force required to shear across adjacent lamellae of the annulus is much larger than that required to induce shearing across fibres within a single lamella[31]. This suggests that bonding across adjacent lamellae, and therefore the proposed mechanism, may be quite important *in vivo*. As a result, the findings of this work may provide key insight into the relationship between form and function in the annulus fibrosus. As the annulus must simultaneously withstand stresses due to axial loading of

the spine as well as torsion, it is possible that the annulus fibrosus is structurally optimized to do so through a combination of collagen fibre stretch and inter-lamellar shearing. This is a unique consequence of its angle-ply organization. Moreover, although inter-lamellar shearing is considered here in the context of the annulus fibrosus and annulus-mimetic engineered tissues, fibre-reinforced laminates are prevalent throughout the body, suggesting that these findings may have implications for other angle-ply laminates, including blood vessels[32], cornea[33], rotator cuff tendon[34], urinary bladder wall, diaphragm and the knee meniscus[35]. To our knowledge, a reinforcement mechanism of the form described here (Fig. 5) has not previously been proposed or investigated for these or other fibre-reinforced biologic laminates. This finding illustrates how biomimetic materials and engineered tissues can serve as simple analogues for complex tissues, providing key insights into the structure–function relationships of their complex native counterparts.

Here, tissue-engineered MSC-derived annulus fibrosus bilayers were formed that, after a period of *in vitro* culture, matched native tissue properties and revealed a novel mechanism of reinforcement in angle-ply biologic laminates. Despite this, it should be noted that the base material used in this work (a slow-degrading polyester) was not optimized for tissue formation. Over the past decade, fervent interest in electrospinning for tissue engineering applications has generated an expanding palette of materials for electrospinning, including biologic polymers that themselves can influence the behaviour of cells and can be manipulated by cells through natural catabolic mechanisms[36–38]. These new materials and their combinations (for example, composites formed by co-electrospinning multiple polymers simultaneously) can produce scaffolds of a wide range of mechanical, structural and degradation characteristics. These materials can be tailored to enhance porosity, mechanics and degradation rates for application-specific properties, and thereby improve tissue formation[39,40]. The use of such methods may further expedite tissue formation based on the angle-ply predicate.

Although the tissue generated in this study replicates the form and function of the annulus fibrosus, there remain several formidable challenges that must be addressed as tissue engineering progresses to clinical implementation for the treatment of damaged or degenerate discs. Translation from the present *in vitro* work to an *in vivo* surgical model will ultimately require integration with the surrounding annular tissue. If loads cannot be effectively transmitted across the engineered–native tissue interface, the engineered tissue will do little to protect the disc from further damage, regardless of its functional properties. MSC-seeded nanofibrous scaffolds do integrate with other fibrocartilaginous tissues *in vitro*[41] and *in vivo*[17]; however, it remains to be determined whether this will occur for the annulus fibrosus under *in vivo* loading conditions. Although in the present work, we matched annulus fibrosus tensile properties, owing to the complexity of the intervertebral disc there is no consensus on what other functional measures must be attained, and to what extent, before proceeding to *in vivo* implantation. As degeneration is thought to initiate from poor nutrient and waste exchange in the largely avascular intervertebral disc, diffusion-limited growth may hamper the scaling of this approach to geometries that are relevant for clinical implementation. Indeed, it is likely that a combination of *in vitro* strategies (such as deformational loading bioreactors to enhance nutrient transfer and tissue deposition) and post-operative measures (such as immobilization to allow integration) will be necessary to overcome these obstacles. Despite these considerable hurdles, this study marks a significant advance in our understanding of biologic laminates such as the annulus fibrosus, and provides a rational approach to the generation of hierarchically and functionally equivalent replacement tissues.

## Methods

**Nanofibrous scaffold fabrication.** Aligned nanofibrous scaffolds were generated by means of electrospinning as described previously[13,19]. Briefly, PCL was dissolved at 143 mg ml$^{-1}$ in equal parts of tetrahydrofuran and N,N-dimethylformamide, then extruded at 2.5 ml h$^{-1}$ through a spinneret charged to +13 kV. The resulting nanofibrous jet was collected on a grounded mandrel rotating at 10 m s$^{-1}$ and located 20 cm from the spinneret. Aluminium shields on either side of the spinneret were charged to +9 kV to focus the jet. The spinneret was fanned back and forth to ensure uniform fibre deposition[39].

**Isolation and seeding of MSCs on nanofibrous scaffolds.** MSCs were isolated from femoral and tibial bone marrow of 3–6 month old calves and expanded to passage 2 as described previously[19]. Scaffolds were hydrated by sequential washes in 100, 70, 50 and 30% ethanol and finally phosphate buffered saline (PBS). Before seeding, scaffolds were incubated overnight in 20 μg ml$^{-1}$ fibronectin. Cell solution (50 μl; $1 \times 10^7$ cells ml$^{-1}$) was applied to one side, followed by incubation at 37 °C for one hour. Scaffolds were then turned and a further 50 μl of cell solution was applied to the other side. After a further two hours incubation, samples were transferred to a chemically defined medium (DMEM, 0.1 μM dexamethasone, 40 μg ml$^{-1}$ L-proline, 100 μg ml$^{-1}$ sodium pyruvate, 1% insulin, transferrin, selenium premix and 1% penicillin, streptomycin and fungizone supplemented with 10 ng ml$^{-1}$ transforming growth factor $\beta$3; ref. 42). The medium was replaced twice weekly for the duration of the study.

**Uniaxial tensile testing and biochemical analyses.** After measuring the cross-sectional area using a custom laser device, samples ($n = 5$) were clamped with serrated grips and loaded into an Instron 5542 testing device[43]. Gauge length was determined as the distance between grips. All testing was carried out in a PBS bath. The mechanical testing protocol consisted of: (1) a nominal tare load of 0.1 N applied at 0.1% strain s$^{-1}$, followed by stress relaxation for 5 min, (2) 15 preconditioning cycles to 0.1% strain at 0.05% strain s$^{-1}$ and (3) a quasi-static elongation at 0.1% strain s$^{-1}$ until failure. Strain was determined as extension normalized to gauge length; stress was computed as the load normalized to initial cross-sectional area. Modulus was computed as the slope of the stress–strain plot, determined by regression to the linear portion of the curve.

For biochemical analyses, samples were digested for 16 h in papain at 60 °C, then analysed for s-GAG content using the 1,9-dimethylmethylene blue dye-binding assay, for orthohydroxyproline (OHP) content (after acid hydrolysis) to determine collagen content by reaction with chloramine T and dimethylaminobenzaldehyde, and for DNA content using the PicoGreen dsDNA Quantification Kit. OHP content was converted to collagen with a ratio of 1:7.14 (OHP/collagen)[42,44].

**Histology.** Samples ($n = 3$) were cryo-sectioned as described previously[13]. Paraformaldehyde-fixed sections were stained for cell nuclei (40,6-diamidino-2-phenylindole, DAPI), glycoasaminoglycans (Alcian Blue) and collagen (Picrosirius Red). DAPI-stained sections were visualized at ×20 on a Nikon T30 inverted fluorescent microscope. Alcian Blue and Picrosirius Red stains were visualized on an upright Leica DMLP microscope. Annulus fibrosus samples from skeletally mature bovine caudal discs were processed identically. Quantitative polarized light microscopy was carried out on Picrosirius Red-stained sections to quantify collagen alignment as described previously[45]. Briefly, greyscale images were collected (×20) at 10° increments using a green band-pass filter (BP 546 nm) with a crossed analyser and polarizer coordinately rotated through 90°. This was repeated with the filter replaced by a λ compensator. Custom software was then used to determine collagen fibre orientations for a series of nodes within the central portion of each region of interest.

**Bilayer lap testing.** Nanofibrous scaffolds of approximately 1 mm thickness were prepared as above and excised along the fibre direction. Two weeks after seeding with MSCs, samples ($n = 5$) were placed in apposition with a 20 mm overlap and secured with porous polypropylene and foil and cultured as above. Lap tests were carried out by gripping the overhang on either end of the bilayer and extending to failure at 0.2 mm s$^{-1}$. Interface strength was determined from the maximum force normalized to overlap area.

**Acellular bilayers.** Aligned nanofibrous scaffolds of approximately 1 mm thickness were excised at 30° from the fibre direction. Agarose was dissolved in PBS at 2, 4, 5 and 6% w/v and melted by autoclaving. Molten agarose was applied between layers of scaffold, and allowed to set at room temperature. No significant difference was observed in cross-sectional area across all concentrations, indicating controlled, reproducible interface formation. Resulting bilayers ($n = 5$) were tested in uniaxial tension as described above.

**Statistics.** Significance was established by $p \leq 0.05$ as determined by two-way analysis of variance with a Tukey's *post hoc* test for independent variables of bilayer orientation (parallel/opposing) and culture duration (or agarose concentration). All data are reported as mean ± s.d. A complete biologic replicate was completed for all experiments, confirming the obtained results.

Received 13 July 2009; accepted 16 September 2009; published online 25 October 2009

## References


1. Cassidy, J. J., Hiltner, A. & Baer, E. Hierarchical structure of the intervertebral disc. *Connect. Tissue Res.* **23,** 75–88 (1989).
2. Elliott, D. M. & Setton, L. A. Anisotropic and inhomogeneous tensile behavior of the human anulus fibrosus: Experimental measurement and material model predictions. *J. Biomech. Eng.* **123,** 256–263 (2001).
3. Hukins, D. W. Tissue engineering: A live disc. *Nature Mater.* **4,** 881–882 (2005).
4. Kandel, R. A., Roberts, S. & Urban, J. Tissue engineering and the intervertebral disc: The challenges. *Eur. Spine J.* **17,** S480–S491 (2008).
5. Place, E. S., George, J. H., Williams, C. K. & Stevens, M. M. Synthetic polymer scaffolds for tissue engineering. *Chem. Soc. Rev.* **38,** 1139–1151 (2009).
6. Mauck, R. L. *et al.* Engineering on the straight and narrow: The mechanics of nanofibrous assemblies for fiber-reinforced tissue regeneration. *Tissue Eng. B* **15,** 171–193 (2009).
7. Chiba, K., Andersson, G. B. J., Masuda, K. & Thonar, E. J. M. A. Metabolism of the extracellular matrix formed by intervertebral disc cells cultured in alginate. *Spine* **22,** 2885–2893 (1997).
8. Thonar, E., An, H. & Masuda, K. Compartmentalization of the matrix formed by nucleus pulposus and annulus fibrosus cells in alginate gel. *Biochem. Soc. Trans.* **30,** 874–878 (2002).
9. Chou, A. I., Reza, A. T. & Nicoll, S. B. Distinct intervertebral disc cell populations adopt similar phenotypes in three-dimensional culture. *Tissue Eng. A* **14,** 2079–2087 (2008).
10. Wan, Y. *et al.* Novel biodegradable poly(1,8-octanediol malate) for annulus fibrosus regeneration. *Macromol. Biosci.* **7,** 1217–1224 (2007).
11. Chang, G., Kim, H. J., Kaplan, D., Vunjak-Novakovic, G. & Kandel, R. A. Porous silk scaffolds can be used for tissue engineering annulus fibrosus. *Eur. Spine J.* **16,** 1848–1857 (2007).
12. Gruber, H. E., Ingram, J. A., Leslie, K., Norton, H. J. & Hanley, E. N. Jr Cell shape and gene expression in human intervertebral disc cells: *In vitro* tissue engineering studies. *Biotech. Histochem.* **78,** 109–117 (2003).
13. Nerurkar, N. L., Mauck, R. L. & Elliott, D. M. ISSLS prize winner: Integrating theoretical and experimental methods for functional tissue engineering of the annulus fibrosus. *Spine* **33,** 2691–2701 (2008).
14. Pittenger, M. F. *et al.* Multilineage potential of adult human mesenchymal stem cells. *Science* **284,** 143–147 (1999).
15. Caplan, A. I. Mesenchymal stem cells. *J. Orthop. Res.* **9,** 641–650 (1991).
16. Marchand, F. & Ahmed, A. M. Investigation of the laminate structure of lumbar disc annulus fibrosus. *Spine* **15,** 402–410 (1990).
17. Li, W. J. *et al.* Evaluation of articular cartilage repair using biodegradable nanofibrous scaffolds in a swine model: A pilot study. *J. Tissue Eng. Regen Med.* **3,** 1–10 (2009).
18. Nerurkar, N. L., Elliott, D. M. & Mauck, R. L. Mechanics of oriented electrospun nanofibrous scaffolds for annulus fibrosus tissue engineering. *J. Orthop. Res.* **25,** 1018–1028 (2007).
19. Baker, B. M. & Mauck, R. L. The effect of nanofiber alignment on the maturation of engineered meniscus constructs. *Biomaterials* **28,** 1967–1977 (2007).
20. Gokorsch, S., Weber, C., Wedler, T. & Czermak, P. A stimulation unit for the application of mechanical strain on tissue engineered anulus fibrosus cells: A new system to induce extracellular matrix synthesis by anulus fibrosus cells-dependent on cyclic mechanical strain. *Int. J. Artif. Organs* **28,** 1242–1250 (2005).
21. Reza, A. T. & Nicoll, S. B. Hydrostatic pressure differentially regulates outer and inner annulus fibrosus cell matrix production in 3D scaffolds. *Ann. Biomed. Eng.* **36,** 204–213 (2008).
22. Neidlinger-Wilke, C. *et al.* A three-dimensional collagen matrix as a suitable culture system for the comparison of cyclic strain and hydrostatic pressure effects on intervertebral disc cells. *J. Neurosurg. Spine* **2,** 457–465 (2005).
23. Mizuno, H. *et al.* Biomechanical and biochemical characterization of composite tissue-engineered intervertebral discs. *Biomaterials* **27,** 362–370 (2006).
24. Smith, L. J. & Fazzalari, N. L. Regional variations in the density and arrangement of elastic fibres in the anulus fibrosus of the human lumbar disc. *J. Anat.* **209,** 359–367 (2006).
25. Stella, J. A. *et al.* Tissue-to-cellular level deformation coupling in cell micro-integrated elastomeric scaffolds. *Biomaterials* **29,** 3228–3236 (2008).
26. Guerin, H. A. & Elliott, D. M. Degeneration affects the fibre reorientation of human annulus fibrosus under tensile load. *J. Biomech.* **39,** 1410–1418 (2006).
27. Huang, A. H., Yeger-McKeever, M., Stein, A. & Mauck, R. L. Tensile properties of engineered cartilage formed from chondrocyte- and MSC-laden hydrogels. *Osteoarthritis Cartilage* **16,** 1074–1082 (2008).
28. Shine, K. M. & Spector, M. The presence and distribution of lubricin in the caprine intervertebral disc. *J. Orthop. Res.* **26,** 1398–1406 (2008).
29. Melrose, J. *et al.* Biglycan and fibromodulin fragmentation correlates with temporal and spatial annular remodelling in experimentally injured ovine intervertebral discs. *Eur. Spine J.* **16,** 2193–2205 (2007).
30. Veres, S. P., Robertson, P. A. & Broom, N. D. ISSLS prize winner: Microstructure and mechanical disruption of the lumbar disc annulus. Part II. How the annulus fails under hydrostatic pressure. *Spine* **33,** 2711–2720 (2008).
31. Michalek, A. J., Buckley, M. R., Bonassar, L. J., Cohen, I. & Iatridis, J. C. Measurement of local strains in intervertebral disc anulus fibrosus tissue under dynamic shear: Contributions of matrix fiber orientation and elastin content. *J. Biomech.* doi:10.1016/j.jbiomech.2009.06.047 (2009).
32. Rhodin, J. in *Handbook of Physiology* (ed. Berne, R.) (Waverly Press, 1980).
33. Maurice, D. M. The structure and transparency of the cornea. *J. Physiol.* **136,** 263–286 (1957).
34. Clark, J. M. & Harryman, D. T. 2nd. Tendons, ligaments, and capsule of the rotator cuff. Gross and microscopic anatomy. *J. Bone Joint Surg. Am.* **74,** 713–725 (1992).
35. Petersen, W. & Tillmann, B. Collagenous fibril texture of the human knee joint menisci. *Anat. Embryol. (Berl)* **197,** 317–324 (1998).
36. Shields, K. J., Beckman, M. J., Bowlin, G. L. & Wayne, J. S. Mechanical properties and cellular proliferation of electrospun collagen type II. *Tissue Eng.* **10,** 1510–1517 (2004).
37. Zhang, X., Baughman, C. B. & Kaplan, D. L. *In vitro* evaluation of electrospun silk fibroin scaffolds for vascular cell growth. *Biomaterials* **29,** 2217–2227 (2008).
38. McManus, M. C., Boland, E. D., Simpson, D. G., Barnes, C. P. & Bowlin, G. L. Electrospun fibrinogen: Feasibility as a tissue engineering scaffold in a rat cell culture model. *J. Biomed. Mater. Res. A* **81,** 299–309 (2007).
39. Baker, B. M. *et al.* The potential to improve cell infiltration in composite fibre-aligned electrospun scaffolds by the selective removal of sacrificial fibers. *Biomaterials* **29,** 2348–2358 (2008).
40. Baker, B. M., Nerurkar, N. L., Burdick, J. A., Elliott, D. M. & Mauck, R. L. Fabrication and modeling of dynamic multi-polymer nanofibrous scaffolds. *J. Biomech. Eng.* doi:10.1115/1.3192140 (2009).
41. Sheth, N. P., Baker, B. M., Nathan, A. S. & Mauck, R. L. *Transactions of the 53rd Annual Meeting of the Orthopaedic Research Society, San Diego, CA* (American Academy of Orthopaedic Surgeons, 2007).
42. Mauck, R. L., Yuan, X. & Tuan, R. S. Chondrogenic differentiation and functional maturation of bovine mesenchymal stem cells in long-term agarose culture. *Osteoarthritis Cartilage* **14,** 179–189 (2006).
43. Peltz, C. D., Perry, S. M., Getz, C. L. & Soslowsky, L. J. Mechanical properties of the long-head of the biceps tendon are altered in the presence of rotator cuff tears in a rat model. *J. Orthop. Res.* **27,** 416–420 (2009).
44. Neuman, R. E. & Logan, M. A. The determination of hydroxyproline. *J. Biol. Chem.* **184,** 299–306 (1950).
45. Thomopoulos, S., Williams, G. R., Gimbel, J. A., Favata, M. & Soslowsky, L. J. Variation of biomechanical, structural, and compositional properties along the tendon to bone insertion site. *J. Orthop. Res.* **21,** 413–419 (2003).


## Acknowledgements

The authors would like to thank J. B. Stambough for assistance with data collection. This work was financially supported by the National Institutes of Health (EB02425), the Aircast Foundation and the Penn Center for Musculoskeletal Disorders (AR050950).

## Author contributions

Experiments were conceived by N.L.N, B.M.B., D.M.E. and R.L.M. Studies on the evolving properties of parallel and opposing bilayers were executed by N.L.N and S.S., with assistance from E.E.W. on histologic analyses. Acellular tensile studies and cell-seeded lap testing studies were carried out by N.L.N. and B.M.B., respectively. The manuscript was prepared by N.L.N., D.M.E. and R.L.M.

## Additional information

Reprints and permissions information is available online at http://npg.nature.com/reprintsandpermissions. Correspondence and requests for materials should be addressed to R.L.M.